

An overview of the ITER EC H&CD system and functional capabilities

M.A. Henderson 1), F. Albajar 2), S. Alberti 3), U. Baruah 4), T. Bigelow 5), B. Becket 1), R. Bertizzolo 3), T. Bonicelli 2), A. Bruschi 6), J. Caughman 5), R. Chavan 3), S. Cirant 6), A. Collazos 3), C. Cox 1), C. Darbos 1), M. debar 7), G. Denisov 8), D. Farina 6), F. Gandini 1), T. Gassman 1), T.P. Goodman 3), R. Heidinger 2), J.P. Hogge 3), S. Illy 12), O. Jean 1), J. Jin 12), K. Kajiwara 9), W. Kasperek 10), A. Kasugai 9), S. Kern 12), N. Kobayashi 9), H. Kumric 10), J.D. Landis 3), A. Moro 6), C. Nazare 1), Y. Oda 9), T. Omori 1), I. Paganakis 3), B. Piosczyk 12), P. Platania 6), B. Plaum 10), E. Poli 11), L. Porte 3), D. Purohit 1), G. Ramponi 6), T. Rzesnick 12), S.L. Rao 4), D. Rasmussen 5), D. Rondén 7), G. Saibene 2), K. Sakamoto 9), F. Sanchez 3), T. Scherer 12), M. Shapiro 13), C. Sozzi 6), P. Spaeh 12), D. Strauss 12), O. Sauter 3), K. Takahashi 9), A. Tanga 1), R. Temkin 13), M. Thumm 12), M.Q. Tran 3), V.S. Udintsev 1), H. Zohm 11) and C. Zucca 3)

- 1) ITER Organization, CS 90 046, 13067 St Paul Lez Durance Cedex, France
- 2) Fusion for Energy, C/ Josep Pla 2, Torres Diagonal Litoral-B3,E-08019 Barcelona – Spain
- 3) CRPP, Association EURATOM-Confédération Suisse, EPFL Ecublens, CH-1015 Lausanne, Suisse
- 4) Institute for Plasma Research, Plot No.A-29, GIDC Electronics Estate, Sector-25, Gandhinagar, 382025, India
- 5) US ITER Project Office, ORNL, 055 Commerce Park, PO Box 2008, Oak Ridge, TN 37831, USA
- 6) Istituto di Fisica del Plasma, Association EURATOM-ENEA-CNR, Milano, Italy
- 7) Association EURATOM-FOM, 3430 BE Nieuwegein, The Netherlands
- 8) Institute of Applied Physics, 46 Ulyanov Street, Nizhny Novgorod, 603950 Russia
- 9) Japan Atomic Energy Agency (JAEA) 801-1 Mukoyama, Naka-shi, Ibaraki 311-0193 Japan
- 10) Institut für Plasmaforschung, Universität Stuttgart, Pfaffenwaldring 31, D-70569 Stuttgart, Germany
- 11) IPP-Garching, Association EURATOM-IPP, D-85748 Garching, Germany.
- 12) Association EURATOM-KIT, IHM and IMF, Postfach 3640, D-76021 Karlsruhe, Germany
- 13) MIT Plasma Science and Fusion Center, Cambridge, MA 02139, USA

E-mail contact of main author: mark.henderson@iter.org

Abstract. A 24MW CW Electron Cyclotron Heating and Current Drive (EC H&CD) system operating at 170GHz is to be installed for the ITER tokamak. The EC system will represent a large step forward in the use of microwave systems for plasma heating for fusion applications; present day systems are operating in relatively short pulses (≤ 10 s) and installed power levels of ≤ 4.5 MW. The magnitude of the ITER system necessitates a worldwide collaboration. This is also reflected in the EC system that is comprised of the power supplies, sources, transmission line and launchers. A partnership between Europe, India, Japan, Russia, United States and the ITER organization is formed to collaborate on design and R&D activities leading to the procurement, installation, commissioning and operation of this system. The aim of this paper is to provide a brief review of the design improvements incorporated in 2008 and 2009 following the ITER design review of 2007. The improvements aim at increased functional capabilities, simplification of interfaces and reduction of procurement and operating risks.

1 Introduction

ITER is planning to install a 24MW Electron Cyclotron (EC) system^[1,2] that will be used for central heating and current drive (H&CD) applications as well as off-axis control of magneto-hydrodynamic (MHD) instabilities. The EC system will be operating at 170GHz for pulse lengths up to 3,600 sec and is comprised of up to 26 gyrotrons, 13 matching high voltage power supplies (HVPS), 24 transmission lines (TL) connected to both one equatorial (EL) and four upper (UL) launchers.

The EC system has undergone significant revisions as a result of the 2007 ITER design review and the subsequent integration of the proposed Project Change Requests (PCRs). The

proposals recommended in the 2007 design review have been reviewed by an international committee of experts, ITER members and DA representatives during the 2008 and 2009 period. Those passing this additional study (managed through the ITER PCR process) have been incorporated into the EC system design.

The 2004 baseline configuration is illustrated in figure 1a, where the power supplies and gyrotrons were located in the assembly hall. This layout had several shortcomings, which included:

- gyrotrons in a high stray magnetic field positioned too close to the tokamak
- high voltage power supplies (HVPS), gyrotrons and transmission lines (TL) installed in the assembly hall could not begin until after the tokamak assembly was completed
- the TL path a large number of mitre bends (9 to 12) increasing transmission losses
- the switching mechanism between the equatorial and upper port launchers was not realistic relative to commercially available mechanisms.

An alternative configuration has been proposed and accepted as illustrated in figure 1b. An RF building is added to house the EC and IC systems (avoids conflict with tokamak assembly), the gyrotrons are positioned further from the tokamak to avoid perturbation from stray magnetic fields and the TL configuration has incorporated commercially available components and follows a path with reduced mitre bends (7 to 9) reducing the cost and improving transmission efficiency.

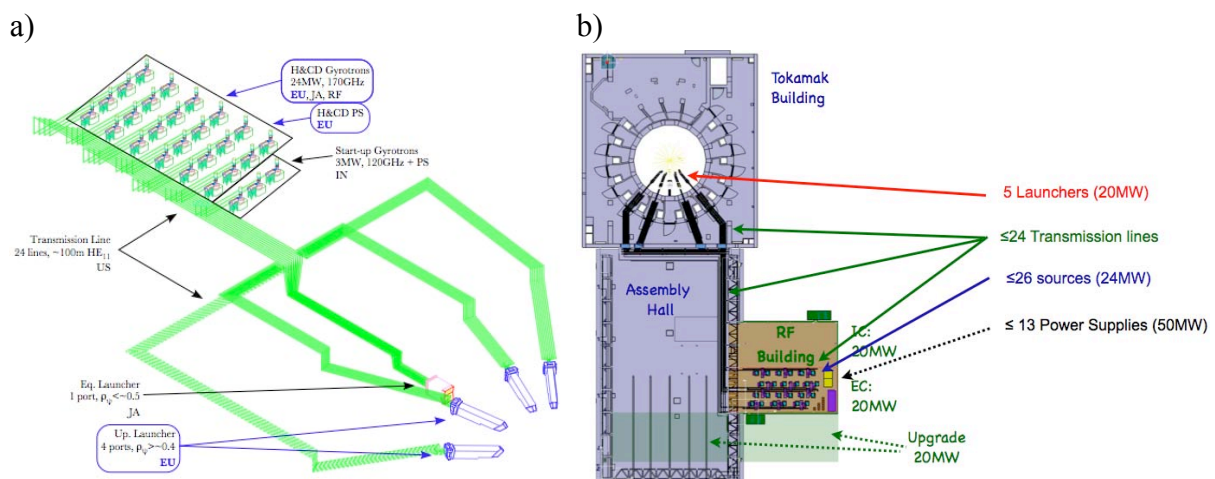


Figure 1. a) The EC system configuration based on the 2004 baseline design, with the HVPS, gyrotrons and part of the TL in the assembly hall. b) The present configuration with the HVPS and gyrotrons in the RF building, the TL following a path from the RF building through the assembly hall to the equatorial and upper launchers in the tokamak building.

The 2007 ITER design review also investigated the functional requirements of the EC system, and modifications were suggested that either improved functionality or simplified the system. The steering ranges of both the equatorial and upper launchers were modified to improve access of the EC system across nearly the entire plasma cross section. Also, the dedicated start-up systems (3MW and frequency near 120GHz) were removed as the 170GHz gyrotron were evaluated as having an equivalent capability for breakdown and burn through at nominal operating regimes.

This paper will provide a brief overview of the changes incorporated since the ITER design review. A preliminary description of the present day system is provided in section 2 below, followed by a review of the functional capabilities of the 170GHz H&CD system.

2 Technical Description

As mentioned above, the EC system is composed of up to 13 main HVPSs, up to 26 gyrotrons, 24 TLs, one equatorial (EL) and four upper (UL) launchers. The gyrotrons will generate 24MW of microwave power, which will then be coupled into the TL and transmitted to either the UL or EL. The overall transmission efficiency is expected to be $\geq 83\%$ such that 20MW will be available for plasma H&CD applications. The overall electrical efficiency is of the order of 40% (20MW divided by the power pulled from the grid). All of these sub-systems, as well as their ancillaries are being procured via in-kind contributions from the Domestic Agencies, which are participating to the construction of the ITER device. The EC system is procured from five of these 7 DAs as outlined in Table 1.

	Europe	India	Japan	Russia	USA
Power Supplies	12 sets	1 set			
Gyrotrons	8MW	2MW	8MW	8MW	
Transmission Lines					24
Launchers	4 UL		1 EL		

In general, the IO is responsible for the functional specifications of all components as well as the built-to-print design of the launchers, the integration management, part of the installation, commissioning and operation. The in-kind procurement strategy taken to build the ITER system requires careful management of the interfaces between each EC sub-system and with interfacing services (such as coolants, vacuum, buildings, etc.)^[3]. The EC sub-systems are to come as a complete package including cabling, control systems, water manifolds, etc, such that all packages fit together without the IO procuring any components. This is illustrated in figure 2 in which the procurement interfaces are defined. The interface between the HVPS and the gyrotrons is at the cable connection near the gyrotron cathode with the HVPS adapting to the voltage and current requirements specified by the gyrotron procurements. Similarly, the interface between the gyrotron and TL is formed at the output of the gyrotron matching optics unit (MOU), with the gyrotron providing a HE₁₁ mode purity of >95% and ≥ 0.96 MW at the waveguide aperture. The end of the TL is at the waveguide connection prior to the diamond window located in either the upper or equatorial port cell. All waveguide components from the diamond window to the plasma are associated with the EL or UL as it forms the primary vacuum and tritium confinement barriers.

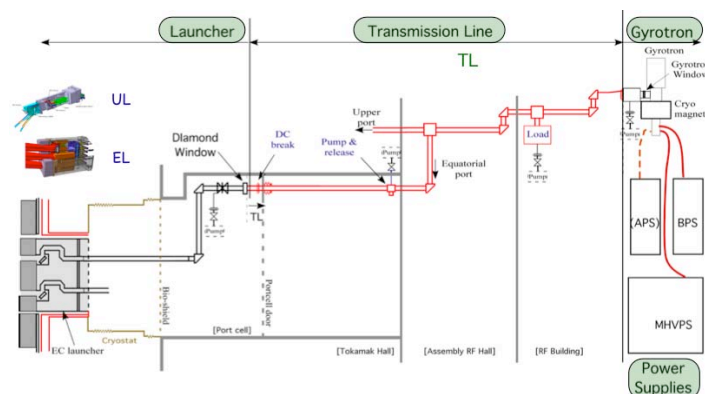


Figure 2. The interface boundaries of the four EC subsystem procurements are at the HV connectors at the gyrotron, the MOU output flange and the waveguide flange on the gyrotron side of the diamond window unit.

2.1 Power Supplies

The HVPS^[4,5] consist of a Main (MHVPS), body (BPS) and (in the case of the triode gyrotrons) anode (APS) HV power supplies. The main parameters of the three HVPS are provided in table 2. Each MHVPS feeds two 1MW (or one 2MW) gyrotron, with a separate BPS (and APS) for each gyrotron. The number of MHVPS was increased from 2 to 12 as a result of the 2007 ITER design review, offering a greater controllability of the delivered power and a more modular design to avoid significant interruption in operation in the event a PS failed.

Table 2 The general parameters of the three HVPS (main, body and anode) used to power the EC gyrotrons.

	Voltage	Current	Modulation	Stability
Main HVPS	55kV	90A	≤1kHz	1%
Body HVPS	~35kV	~200mA	≤5kHz	1%
Anode HVPS	~40kV	~50mA	≤5kHz	1%

All power supplies are envisioned to use the Pulse Step Modulated (PSM) design that offers fine control and high frequency modulation (≤5kHz) of the applied voltage. The HVPS are configured on the bottom two floors of the RF building as shown in figure 3. The MHVPSs are on the first level, followed by the BPSs (and APSs) on the second level, all of which are directly below the gyrotrons on the third level. The vertical configuration minimizes the cable length between the supplies and gyrotrons, thus reducing the stored energy in the cable. The configuration also simplifies the building design keeping the heavier items (in particular the MHVPS transformers) on the ground floor and leaving the ceiling of the third floor relatively high for lifting the gyrotrons with an overhead crane.

Note that the RF building size is compatible with a 24MW EC system, which is predominately limited by the space required for 12 power supplies (rather than the 13 planned in the in-kind procurement sharing). The building size also limits the number of gyrotrons to 24 (assuming all 1MW sources) or 20 (assuming four 2MW sources).

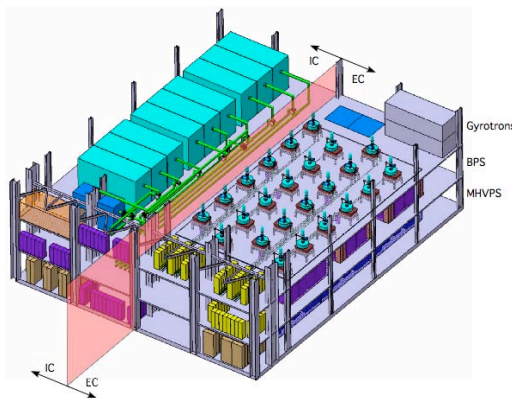


Figure 3. The RF building (B15) houses the IC and EC systems, which are each distributed on three floors. The first two floors are for PS and the top floor for the sources.

2.2 Gyrotrons

The gyrotrons^[6-10] are to be provided by four DAs as outlined in Table 3, with the gyrotron type varying with each procurement. The general gyrotron specifications are to generate ≥0.96MW at the MOU output (≥1.0MW at the window) and >95% coupling to the HE₁₁ mode. The gyrotron procurement includes a Helium free cryomagnet, MOU, cooling manifold, local control system, support structure and ancillary systems. The tube should have an electrical efficiency of ≥50%.

The gyrotrons will be distributed on a grid with typically ≥4m spacing and an equivalent distance between building iron structures (see figure 3). The spacing is maximized within the finite size of the building to minimize impact on each gyrotron’s magnetic field. All gyrotrons

are positioned $>90\text{m}$ from the tokamak center limiting the horizontal component of the stray field to $\leq 3\text{mT}$ along the electron beam trajectory. Note that since the 2004 EC system design, the MOU has been included into the gyrotron package and the function of the polarizer mirrors and calorimetric load transferred to the TL (these functions are available with standard commercial components).

	Power	Cavity	Gun	Reference
EU-DA	2.0MW	Co-axial	diode	[9,10]
IN-DA	1.0MW	cylindrical	TBD	[8]
JA-DA	1.0MW	cylindrical	triode	[6]
RF-DA	1.0MW	cylindrical	diode	[7]

2.3 Transmission Lines

The TL ^[11,12] has the primary function of transmitting the EC power from the gyrotrons up to the launcher diamond windows in the equatorial and upper port cells. The overall transmission efficiency should be $\geq 90\%$ with a maximum degradation of the HE_{11} content of 97% relative to the mode purity at the output of the MOU. The transmission line performs additional functions, which include:

- Monitor forward and reflected power (using power monitor mitre bend)
- Deviate power to dummy load (via an in-line switch)
- Modify beam polarization for optimum plasma coupling
- Deviate power to either upper or equatorial launchers via in-line automatic switches
- Provide pumping access for maintaining low pressure in line
- Electrically isolate line from gyrotron and launchers

The components achieving these functionalities are distributed in a typical TL illustrated in figure 4. The TL is formed from evacuated 63.5mm HE_{11} aluminium waveguide ^[13], equivalent to the waveguide used on TCV ^[14] and Tore Supra ^[15] but with a different frequency bandwidth and designed for 2MW steady state operation. High power long pulse testing of equivalent waveguide components are ongoing at JAEA ^[16].

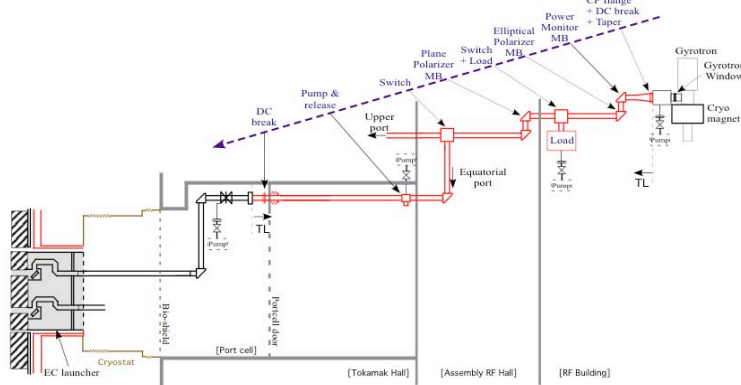


Figure 4. The principle components are shown between the MOU and diamond window for a generic TL.

The layout of the TL has been changed from 2004 as a result of the change in PS/gyrotron location as well as a reconfiguration of the layout to minimize the number of mitre bends from typically 9-12 to 7-9. Note that the mitre bend is the primary source of transmission losses, which are minimized to increase the available power to the plasma. The 2004 design was pre-conceptual with few waveguide components consistent with commercially available designs. In revising the TL layout, waveguide components equivalent to what is available from industry and what is being tested at the JAEA test bed ^[16] were used to ensure compatibility with industrial standards.

2.4 Launchers

ITER requires two types of launchers to achieve the functional requirements desired for the EC H&CD system: central H&CD and the off-axis CD for controlling MHD activity. These functions are distributed between the equatorial (EL)^[17,18] and upper (UL)^[19-21] launchers, respectively, which are shown in figure 5a and b. Both launchers are to be compatible with 1.8MW beams, consistent with the possible 2MW gyrotron procurement from the EU and assuming 10% transmission losses from the MOU and TL.

Changes that have been incorporated resulting from the 2007 ITER design review include:

- Revision of the primary confinement system
- Modification of the EL and UL steering range for improved accessibility^[22]
- Simplification of the EL and UL by replacing internal mitre bends with free space mirrors
- Modifying the EL toroidal steering angles of 8 beams for counter injection.

These modifications are briefly described herein and in the following section.

The primary confinement system has been revised since the 2004 design, with the isolation valve now located on the plasma side of the diamond window providing increased maintenance access and in-situ leak testing of the window independent of the torus pressure. The valve and window have been placed outside the bio-shield for increased accessibility. The torus displacements ($\leq \pm 30\text{mm}$) will be compensated with the elastic bending of approximately 10m of waveguide and two mitre bends. Note that the torus will displace due to temperature variations, plasma disruptions, thermal quenches and loss of coolant. The waveguides will be aligned during nominal operating conditions (to minimize mode conversion losses) and then deflect as the torus displaces.

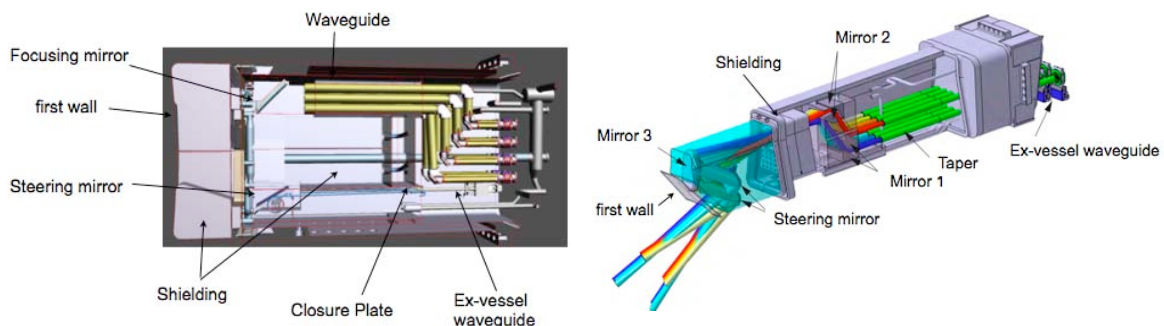


Figure 5. A) The equatorial launcher cut in a horizontal plane showing the waveguide orientation, focusing mirror, steering mirror, port plug structure and blanket modules. B) The upper launcher cut in a vertical plane showing the waveguide orientation, three fixed mirror sets, two steering mirrors, port plug structure and blanket module.

The equatorial launcher has a total of 24 beams at the entry, which are grouped into three sets of eight beams. Each beam set is projected to a focusing then flat steering mirror before passing through the blanket shield module (BSM) and into the plasma. Previously, the beams were steered from 20 to 45°, however this is now limited to 41° to avoid increased stray radiated power in the torus. Non-negligible amounts of shine through power occur from the EL when the angle exceeds 42°. A slight poloidal tilt has also been introduced such that all three EL steering mirrors can access from near on-axis to $\rho_T \leq 0.45$ (plasma coordinates, where ρ_T is the square root of the normalized toroidal flux). This ensures the EC system can heat and drive current centrally from any steering mirror. Previously, only one mirror had central access, if that mirror failed, the EC system would have lost access inside of $\rho_T \leq \sim 0.2$.

The upper launchers have also been modified, with an increased steering range accessing from $0.3 \leq \rho_T \leq \sim 0.95$ as compared to the 2004 design of $0.5 \leq \rho_T \leq \sim 0.85$. This has been achieved

by spreading out the access range of the two steering mirrors inside the UL. In each of the four ULs, there are eight waveguide entries grouped into two sets of four beams. The beams propagate in free space through a set of four mirrors that regroup and focus the beams to provide a narrow and peaked current density profile for control of the MHD instabilities. The last mirror is a steering mirror that injects the beam over a poloidal range of $\pm 12^\circ$ to access the relevant $q=2$ and $3/2$ rational flux surfaces. The top steering mirror aims closer to the plasma center to access in to $0.3 \leq \rho_T$, while the lower steering mirror aims further upward to access out to the plasma edge $\rho_T \leq \sim 0.95$. Note that the beams have a nearly fixed toroidal injection angle of about 20° that provides a maximized peak current density profile over the desired access range.

3 Functional Description

As mentioned above, the changes in the steering angles of the EL and UL have improved the accessibility of the EC system for H&CD applications across nearly the entire plasma cross section. The original baseline design (prior to 2007) partitioned the physics applications between the two launchers based on regions in the plasma. The EL accessing inside of $\rho_T \leq \sim 0.45$ for applications associated with central heating, current drive and sawtooth control and the UL accessing only the region where NTMs are expected to occur between $\sim 0.55 \leq \rho_T \leq \sim 0.85$. The combination of two launchers could not achieve the desired accessibility.

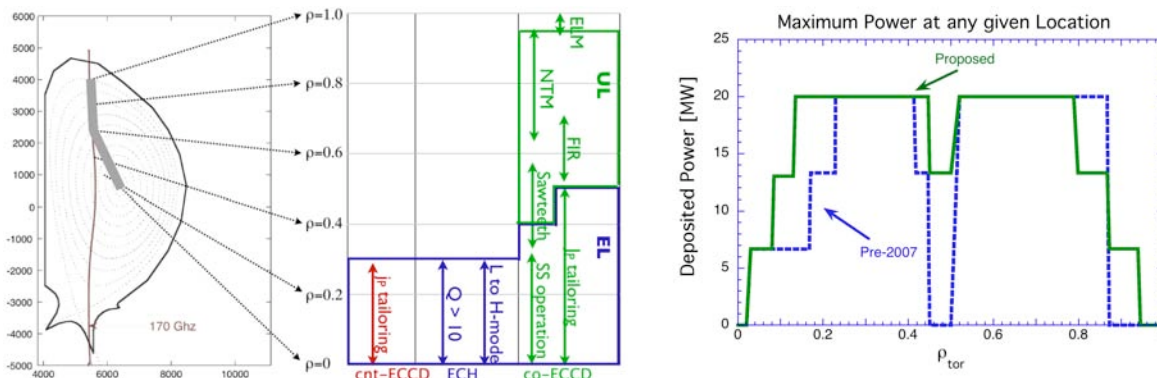


Figure 6. A) The revised equatorial and upper launchers access nearly the entire plasma cross section and are capable of injecting 20MW in the co-ECCD direction, 6.7MW in the counter-ECCD, or a balanced injection of the full 20MW for effectively pure heating. B) The maximum power that can be deposited at any given location in the plasma cross section based on the pre-2007 design (blue dashed line) and today’s configuration (green solid line).

The design teams have modified the launcher designs increasing the access range and avoiding regions of non-accessibility (as shown in figure 6) by increasing the access range of the UL. The physics applications have been repartitioned between the two launchers^[22], dividing the functional requirements based on the need for broad (EL) or narrow (UL) deposition profiles. The EL would still be used for central heating and current drive applications^[23], while the UL used for the control of both the NTM and sawtooth instabilities. In addition, one third of the EL beams are to provide counter current drive to decouple the heating and current drive contributions when depositing power centrally.

4 Schedule

The EC system is envisioned to provide 8MW (installed) for the first ITER plasma scheduled in late 2019 and the full 24MW (installed) for the second operating period in 2022. The design, manufacturing, installation and commissioning activities are configured according to these milestones with some margin of float (typically \geq one year) prior to the planned plasma

initiation date. The installation process will begin in mid 2015 after the RF, assembly and Tokamak buildings are available for EC equipment installation. The installation strategy is to install and commission a power supply in parallel with the corresponding gyrotron installation. Once the power supply is accepted, the gyrotron commissioning and acceptance will follow. A second PS will be installed and commissioned along with the installation of a second set of gyrotrons, while the first set of gyrotrons is being accepted. This procedure of parallel activities will continue into all PS and gyrotrons are installed (in 2019). The TL and launchers are envisioned to be installed in parallel with the PS and gyrotrons depending on the access availability to the assembly hall and tokamak buildings. All launchers will be installed for the 2021 plasma operation. The requirements for the 2019 first plasma operation is under study, with the possibility of a simplified launcher to be introduced for assisting plasma start-up (initiation and burn-through).

5 Summary

The EC system has undergone a series of modifications arising from the 2007 ITER design review. These modifications were proposed with the aim of increasing functionality, improving interface management, simplifying component design based on known industrial capabilities and reduction of risks associated with potential technical and schedule issues. The modifications have impacted all aspects of the EC system design including the power supplies, gyrotrons, TL, launchers, the interfaces between these subsystems and their functional capabilities. All of these modifications were introduced following the ITER Project Change Request, which includes review of all proposals by external technical experts, interfacing systems and the impacted DAs.

References

1. M. Henderson et al, *An Overview of the ITER EC H&CD System*, IRMMW-THz Conference, 21-25 Sept. 2009, Busan, Korea.
2. C. Darbos et al, *ECRH system for ITER*, RF conference, June 2009, Gent, Belgium.
3. M. Henderson and G. Saibene, *Nucl. Fusion* **48** (2008) 054017.
4. D. Fasel et al, *Fusion Sci. Technol.* **53** (2008) 246.
5. T. Gassmann et al, *Integration of IC /EC systems in ITER* ISFNT-09 conference, October 11-16, 2009, Dalian, China.
6. K. Sakamoto et al *Nature* **3** (2007) 411.
7. G. Denisov et al *Recent Development Results in Russia of Megawatt Power gyrotrons for Plasma Fusion Installations*, this Conf.
8. S.L. Rao et al, "Design Change, its Implications & Alternate Options for the EC Source System for ITER Plasma Start-Up", 5th IAEA TM on "ECRH Physics & Technology for Large Fusion Devices", 18-20 Feb. 2009, Gandhinagar, INDIA.
9. F. Albajar et al, *The European 2MW gyrotron for ITER*, this Conf.
10. J.-P. Hogge et al, "First experimental results from the European Union 2-MW coaxial cavity ITER gyrotron prototype," *Fus. Sci. Technol.*, vol. 55, no. 2, pp. 204-212, Feb. 2009..
11. D. Rasmussen et al *R&D Progress on the ITER EC Transmission Line*, this Conf.
12. F. Gandini et al, *An Overview of the ITER EC Transmission Line*, this Conf.
13. R.A. Olstad, J.L. Doane, and C.P. Moeller, *Fusion Engineering and Design* **74**, no. 1 (November 2005): 331-335.
14. T.P. Goodman et al, *Proc. of the 19th Symposium on Fusion Technology Lisbon Portugal (1996)* p 565.
15. M. Lennholm et al, *Nucl. Fusion* **43** (2003) 1458-1476.
16. K. Takahashi et al., *Proc. 8th International Vacuum Electronics Conference*, Kitakyushu, Japan, 2007.
17. K. Takahashi et al *Nucl. Fusion* **48** (2008) 054014.
18. K. Kajiwara et al, *Fusion Engineering and Design* **84** (2009) 72-77
19. D. Strauss et al, *Deflections and Vibrations of the ITER ECRH Upper Launcher*, this Conf.
20. T. Scherer et al, *Recent Upgrades of the ITER ECRH CVD Torus Diamond Window Design and Investigation of Dielectric Diamond Properties*, this Conf.
21. M. Henderson et al *Nucl. Fusion* **48** (2008) 054013.
22. G. Ramponi et al, *Nucl. Fusion* **48** (2008) 054012.
23. C. Zucca et al, *Theory of Fusion Plasmas AIP Conf. Proc.* **1069** (2008) 361